

# Interfacial Activity of Gradient Copolymers

Kenneth R. Shull

Department of Materials Science and Engineering, Northwestern University,  
Evanston, Illinois 60208-3108

Received May 6, 2002

**ABSTRACT:** Numerical self-consistent field (SCF) theory is used to study the equilibrium segregation of A/B gradient copolymers to the interface between immiscible A and B homopolymers. A generalized SCF theory is developed that allows arbitrary composition gradients to be investigated. The focus of this paper is on symmetric copolymers consisting of equal amounts of A and B repeat units, with a linear or hyperbolic tangent composition gradient. A gradient parameter,  $\lambda$ , is introduced that describes the length of the composition gradient relative to the length of the entire copolymer molecule. Critical values of the copolymer chemical potential corresponding to the formation of copolymer micelles, or to a vanishing interfacial free energy between A and B homopolymer phases, decrease with  $\lambda$ , and are about  $1.6k_B T$  lower for  $\lambda = 1$  than for  $\lambda = 0$ . The width of the concentration profile of A or B repeat units within a lamellar copolymer phase, or across an emulsified interface, increases with  $\lambda$ , and is equal to about twice the copolymer radius of gyration for  $\lambda = 1$ .

## 1. Introduction

The ability of block copolymers to segregate to the interface between immiscible homopolymers, modifying the interfacial structure and reducing the interfacial tension, is well documented.<sup>1–3</sup> The interfacial activity is determined by a relationship between the interfacial copolymer excess,  $\nu_c$  (expressed in molecules per unit area), and the copolymer chemical potential  $\mu_c$ . The maximum copolymer chemical potential is determined by the formation of lamellar, spherical, or cylindrical micelles, which in some cases aggregate to form the bulk structures with the corresponding symmetries.<sup>4,5</sup> The thermodynamic stability of these different bulk structures is determined by the copolymer composition and by the overall thermodynamic incompatibility between the two blocks. In the absence of homopolymer, one obtains the well-known phase map where the different morphologies (spherical, cylindrical, bicontinuous, or lamellar) are determined by the values of  $f$  and  $\chi N_c$  that characterize the copolymer of interest.<sup>5</sup> Here  $N_c$  is the total number of repeat units along an A/B diblock copolymer molecule,  $f$  is the fraction of these repeat units corresponding to the A species, and  $\chi$  is the Flory parameter characterizing the thermodynamic interactions between A and B repeat units. Addition of homopolymer shifts the morphology map in a manner that is determined by the relative molecular weights of the homopolymer and the corresponding copolymer block.<sup>6–9</sup> If the homopolymer composition is identical to the A copolymer block, then the relevant molecular weight ratio is  $fN_c/N_h$ . For values of this quantity less than approximately 1, the homopolymer does not substantially affect the symmetry of the micellar aggregates. In these cases the geometry of the micellar aggregates is adequately described by the same phase map used to describe the morphology of a pure diblock copolymer melt.

Through recent advances in “living” radical polymerization methods, including atom transfer radical polymerization<sup>10–12</sup> and nitroxide-mediated polymerization,<sup>13–15</sup> it is now possible to synthesize a wide variety of “gradient” copolymers, where the average

composition of the molecules varies in a controlled fashion from one end of the molecule to another. The aim of this paper is to introduce a theoretical formalism for investigating the ability of these materials to modify the properties of homopolymer interfaces and to provide some insight into the unique features of these materials in comparison to traditional diblock copolymers. The focus of this paper is on simple A/B systems, where the thermodynamic interactions are described by a single value of  $\chi$ . The local volume fraction of A repeat units along the backbone of the copolymer chains is described by the function  $g(n)$ , where  $n$  is an index that varies from 0 at one end of the copolymer chain to  $N_c$  at the other end of the chain. The overall composition,  $f$ , is given as the average value of  $g$ :

$$f = \frac{1}{N_c} \int_0^{N_c} g(n) \, dn \quad (1)$$

To illustrate the general behavior of gradient copolymers, the discussion here is restricted primarily to polymers with linear gradients with  $f \geq 0.5$ , in which case it is useful to express  $g(n)$  in the following way:

$$\left[ \begin{array}{ll} g(n) = 1 & \frac{n}{N_c} < f - \lambda(1 - f) \\ g(n) = 0.5 + \frac{1}{2\lambda(1 - f)} \left( f - \frac{n}{N_c} \right) & f - \lambda(1 - f) < \frac{n}{N_c} < f + \lambda(1 - f) \\ g(n) = 0 & \frac{n}{N_c} > f + \lambda(1 - f) \end{array} \right] \quad (2)$$

The parameter  $\lambda$  expresses the length of the composition gradient relative to the length of the B copolymer block, which is assumed here not to exceed the length of the A copolymer block. For  $\lambda = 0$ , the copolymer is a traditional block copolymer consisting of  $fN_c$  A units followed by  $(1 - f)N_c$  B units. For  $\lambda = 1$ , the composition varies smoothly from pure B for  $n = N_c$  to pure A for  $f < (2f - 1)N_c$ . The discussion here is restricted to values of  $\lambda$  between 0 and 1, corresponding to the range of gradients for which eq 2 is valid. Values of  $g(n)$  are plotted in Figure 1 for  $f = 0.5$  and  $\lambda = 0, 0.5$ , and 1.

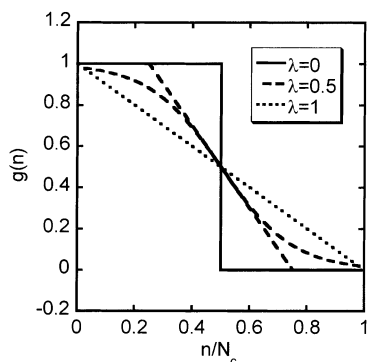


**Figure 1.** Definition of  $\lambda$ .

To verify that results obtained for different values of  $\lambda$  are somewhat representative, the following hyperbolic tangent form of  $g(n)$  has also been considered in some cases:

$$g(n) = 0.5 + 0.5 \tanh\left(\frac{2(f - n/N_c)}{\lambda}\right) \quad (3)$$

The central region of this profile is identical to the linear profile with the same value  $\lambda$ . This similarity is illustrated in Figure 1, which includes the tanh profile for  $\lambda = 0.5$ . Also, note that  $f'$  is equal to  $f$  when  $f'$  is equal to 0.5 (all the cases considered in this paper), or for values of  $f'$  that are small enough so that  $g(0) \approx 1$  and  $g(N_c) \approx 0$ . Copolymers with composition gradients given by eq 2 are referred to as linear gradient copolymers throughout the remainder of this paper, whereas those with composition gradients given by eq 3 are referred to as tanh gradient copolymers.

## 2. Theoretical Formulation

The thermodynamic model of copolymer interactions begins with the Flory–Huggins expression for the free energy of mixing, and the chemical potential expressions that are derived from this free energy expression. In this model, the free energy per unit volume,  $\Delta f$ , of a homogeneous mixture of monodisperse A and B homopolymers is given by the following familiar expression

$$\Delta f = \frac{k_B T}{v_0} \left\{ \frac{\phi_a \ln \phi_a}{N_a} + \frac{\phi_b \ln \phi_b}{N_b} + \chi \phi_a \phi_b \right\} \quad (4)$$

where  $N_a$  and  $N_b$  are the molecular volumes, normalized by a reference volume,  $v_0$ , that is typically taken as the volume of one of the polymer repeat units. Note that the interaction parameter  $\chi$ , is defined in terms of this same reference volume. The chemical potential for A homopolymer chains in a homogeneous mixture of A and B chains is given by the following expression<sup>16</sup>

$$\frac{\mu_a}{k_B T} = \ln \phi_a + \phi_b \left(1 - \frac{N_a}{N_b}\right) + \mu_\chi \quad (5)$$

with

$$\mu_\chi = \chi N_a \phi_b^2 = \chi N_a (1 - \phi_a)^2 \quad (6)$$

The first two terms in eq 5 are the ideal entropy of mixing terms. The enthalpy of mixing, and any nonideal entropy of mixing, is included in  $\mu_\chi$ .

The need here is for a generalization of eq 6 to the case where the A polymer is replaced by a statistical

copolymer of A and B repeat units, where  $g$  is the volume fraction of A repeat units in the copolymer. A course-grained approach is used that ignores the detailed sequence distribution of the different types of repeat units, focusing only on the average local composition,  $g$ . The problem is equivalent to a calculation of the effective value of  $\chi$  between a statistical A/B copolymer with a composition of  $g$  (representing the copolymer composition) and a statistical A/B copolymer with a composition of  $\phi_a$  (representing the overall composition of the matrix to which a single copolymer molecule is added). Simple Flory type arguments give a value for this effective  $\chi$  that depends on the square of the composition difference between the copolymers:<sup>17,18</sup>

$$\chi_{\text{eff}} = \chi (g - \phi_a)^2 \quad (7)$$

Because the copolymer with a composition of  $\phi_a$  represents the composition of the matrix into which the copolymer chains are added, one can calculate  $\mu_\chi$  by setting  $\phi_b$  to 1 in eq 6 and replacing  $\chi$  with  $\chi_{\text{eff}}$ :

$$\mu_\chi = \chi_{\text{eff}} N_c = \chi N_c (g - \phi_a)^2 \quad (8)$$

$N_a$  has been placed with  $N_c$  to indicate that the molecule of interest is now a statistical copolymer. Note that eq 6 is a special case of eq 8, with  $g = 1$ .

The quantity  $\mu_\chi/N_c$  represents the average contribution to  $\mu_\chi$  from each segment of the polymer chain. In the case where the composition varies along the chain, as in a gradient copolymer, these contributions must be integrated to give the value of  $\mu_\chi$ :

$$\mu_\chi = \chi \int_0^{N_c} (g(n) - \phi_a)^2 dn \quad (9)$$

The chemical potential for a gradient copolymers of degree of polymerization  $N_c$  in an A homopolymer matrix with degree of polymerization  $N_h$  is obtained by adding the ideal entropy of mixing terms from eq 5:

$$\frac{\mu_c}{k_B T} = \ln \phi_c + \phi_h \left(1 - \frac{N_c}{N_h}\right) + \chi \int_0^{N_c} (g(n) - \phi_a)^2 dn \quad (10)$$

In this case  $\phi_a$  is the overall volume fraction of A repeat units, including repeat units from the A homopolymer and from the gradient copolymer,  $\phi_c$  is the copolymer volume fraction, and  $\phi_h$  is the volume fraction of homopolymer chains.

For heterogeneous systems, the local volume fractions are obtained by solving a set of mean-field equations.<sup>19</sup> The central quantities are probability distribution functions that characterize molecular configurations as random walks that are perturbed by a spatially dependent mean field. For a multicomponent system, each polymer component,  $k$ , is characterized by two distribution functions,  $q_{k1}$  and  $q_{k2}$ . These functions characterized the two chain ends of a given polymer component, and obey modified diffusion equations of the following form:

$$\begin{aligned} \frac{\partial q_{k1}(\mathbf{r}, n)}{\partial n} &= \frac{a^2}{6} \nabla^2 q_{k1}(\mathbf{r}, n) - \omega_k(\mathbf{r}, n) q_{k1}(\mathbf{r}, n) \\ \frac{\partial q_{k2}(\mathbf{r}, n)}{\partial n} &= \frac{a^2}{6} \nabla^2 q_{k2}(\mathbf{r}, n) - \omega_k(\mathbf{r}, N_k - n) q_{k2}(\mathbf{r}, n) \end{aligned} \quad (11)$$

where  $a$  is the statistical segment length of a repeat unit and  $\omega_k$  is a thermodynamic field acting on each repeat unit.<sup>20</sup> The two distribution functions describe possible configurations of the molecule on either side of a junction located along the polymer chain backbone. Volume fractions are obtained by summing over all possible junction points:

$$\begin{aligned}\phi_{ka}(\mathbf{r}) &= \exp\left(\frac{\mu_k}{k_B T} - 1\right) \int_0^{N_k} g_k(n) q_{k1}(\mathbf{r}, n) q_{k2}(\mathbf{r}, N_k - n) \, dn \\ \phi_{kb}(\mathbf{r}) &= \exp\left(\frac{\mu_k}{k_B T} - 1\right) \int_0^{N_k} (1 - g_k(n)) q_{k1}(\mathbf{r}, n) q_{k2}(\mathbf{r}, N_k - n) \, dn\end{aligned}\quad (12)$$

Note that each component is characterized by its own composition function,  $g_k$ . The overall volume fractions of A and B repeat units are obtained by summing the contributions from each of the components:

$$\phi_a(\mathbf{r}) = \sum_k \phi_{ka}(\mathbf{r}), \quad \phi_b(\mathbf{r}) = \sum_k \phi_{kb}(\mathbf{r}) \quad (13)$$

The fields depend on the average local composition of the surroundings, and on the composition of the component in question. As described in the Appendix, the field expressions can be written in a variety of equivalent ways. The form here is based on the chemical potential expressions, and is expressed as follows

$$\omega_k(\mathbf{r}, n) = \chi(g_k(n) - \phi_a(\mathbf{r}))^2 - \sum_k \frac{\phi_k(\mathbf{r})}{N_k} - \Delta\omega(\mathbf{r}) \quad (14)$$

where  $\Delta\omega(\mathbf{r})$  can be viewed as an excess negative pressure that enforces the requirement that the volume fractions of the different components sum to unity. Integration of this component gives the interfacial free energy,  $\gamma$ . For a flat interface, where the spatial dependence of the quantities in the above equations is a function of  $z$ , the distance from the interface, one has<sup>21</sup>

$$\gamma = \frac{ak_B T}{v_0} \int_{-\infty}^{\infty} \Delta\omega(z) \, dz \quad (15)$$

By taking the incompressible limit, one assumes that the negative excess pressure represented by the quantity  $k_B T \Delta\omega/v_0$  is not sufficient to change the density of the material, that is,  $v_0$  is a constant. Any tendency for the more compressible components to segregate preferentially to the interface as a result of this negative interfacial pressure is neglected,<sup>22</sup> as are chain end effects<sup>23</sup> and structural detail at the level of the repeat unit which determine the detailed temperature and composition dependence of  $\chi$ .<sup>24</sup> Here  $\chi$  is treated as a phenomenological parameter that is operationally defined by the chemical potential expression (eqs 5 and 6). The relatively large values of  $\chi$  that are of interest for gradient copolymers can be obtained experimentally by a variety of methods, including determination of the coexistence curves for immiscible homopolymers<sup>25</sup> and measurement of the equilibrium interfacial segregation of a standard diblock copolymer.<sup>3</sup>

Solution of discretized versions of the self-consistent-field equations in spherical, cylindrical, or planar coordinates can be used to determine the properties of the corresponding micellar geometries.<sup>26</sup> Values of  $\mu_{\text{cmc}}$ , the copolymer chemical potential for chains in an equilibrium micelle, and the corresponding values of the critical micelle concentration are determined from the requirement that the overall free energy change due to the formation of a micelle is 0:

$$\int \Delta\omega(\mathbf{r}) \, d\mathbf{r} = 0, \quad \text{for } \mu_c = \mu_{\text{cmc}} \quad (16)$$

In contrast to the Landau–Ginzburg formalism that has been applied to studies of the order/disorder transitions of traditional diblock copolymers,<sup>27</sup> and more recently to gradient copolymers,<sup>28</sup> the validity of the SCF formalism is not restricted to the weak segregation regime. In fact, the SCF treatment can often be applied quantitatively in systems that are well removed from any critical points,<sup>19</sup> where fluctuation corrections to the underlying mean-field treatment<sup>29–31</sup> are not important. An additional assumption that remains within the present implementation of the SCF treatment is that the gradient portion of the copolymers are not too “blocky”; there are no sequences of A or B repeat units that are sufficiently long to result in microphase separation.<sup>31,32</sup> This condition is relatively easy to meet by appropriately choosing the monomer feed ratios during the polymerization of the gradient polymers.<sup>33,34</sup> Even in this case, however, there will be a distribution of compositions around the average value, and the collection of gradient copolymers is formally a multicomponent mixture. Replacing these different components with a single “average” component is an additional approximation that is not a relevant consideration in treatments of traditional diblock copolymers, where all of the molecules have essentially the same composition. The remarkable ability of SCF theory to provide quantitatively accurate predictions for the adsorption isotherms of diblock copolymer molecules at homopolymer interfaces,<sup>3,35</sup> including the end point corresponding to the formation of block copolymer micelles,<sup>26</sup> may not be preserved as the gradient parameter is increased toward  $\lambda = 1$ . Nevertheless, the qualitative conclusions described in the following section are expected to provide useful guidelines for designing gradient copolymers with the desired interfacial properties.

### 3. Results and Discussion

For relatively large values of the homopolymer molecular weight ( $N_c/N_h < 1$ ), the copolymer exists as an interfacial layer that is not strongly swollen by the homopolymer.<sup>20</sup> Similarly, the outer corona blocks of the block copolymer micelles are not significantly swollen by the surrounding homopolymer. In this case  $\mu_{\text{cmc}}$ , the copolymer chemical potential at the critical micelle concentration, is accurately given by the following analytic approximation:<sup>26</sup>

$$\frac{\mu_{\text{cmc}}}{k_B T} = 1.16(\chi N_c)^{1/3} h(f) + 0.55 \ln(\chi N_c) - 0.76 \quad (17)$$

where  $h(f)$  is equal to 1 for  $f = 0.5$  and decreases for larger values of  $f$ . (Recall that  $f$  corresponds to the volume fraction of the corona-forming block in this paper.) The functional form of  $h(f)$  is different for



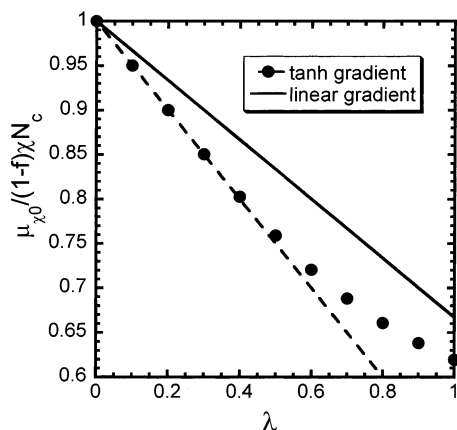


**Figure 2.** Values of  $\mu_{\chi 0}$  for copolymers with linear and tanh gradients.

lamellar, cylindrical, and spherical micelles. For  $f = 0.5$ , the lamellar micelles considered in this paper have the lowest value of  $h(f)$  and are thermodynamically preferred in comparison to the other geometries.

The volume fraction of free, unassociated copolymer molecules in equilibrium with the micellar aggregates can be obtained from equating  $\mu_{\text{cmc}}$  with the chemical potential for free chains. In the dilute limit ( $\phi_a \rightarrow 1$ ), eq 10 reduces to the following expression for the chemical potential of these free chains in terms of  $\phi_{\text{bulk}}$ , their volume fraction in the bulk B phase

$$\frac{\mu_c}{k_B T} = \ln \phi_{\text{bulk}} + \phi_h \left( 1 - \frac{N_c}{N_h} \right) + \mu_{\chi 0} \quad (18)$$

with

$$\mu_{\chi 0} = \chi \int_0^{N_c} (g(n) - 1)^2 dn \quad (19)$$

Note that  $k_B T \mu_{\chi 0}$  is the free energy (excluding the ideal entropy of mixing) required to add a single copolymer molecule to the A homopolymer matrix.

The value of  $\phi_{\text{cmc}}$ , the volume fraction of free copolymer chains in equilibrium with copolymer micelles, is obtained by setting  $\mu_c = \mu_{\text{cmc}}$  and  $\phi_{\text{bulk}} = \phi_{\text{cmc}}$  in eq 18 and rearranging. For  $N_c/N_h = 1$  one obtains:

$$\ln(\phi_{\text{cmc}}) = \frac{\mu_{\text{cmc}}}{k_B T} - \mu_{\chi 0} \quad (20)$$

For linear gradients with  $\lambda \leq 1$ , the integral for  $\mu_{\chi 0}$  can be solved analytically to give the following:

$$\mu_{\chi 0}(\text{linear}) = \chi(1 - f)N_c \left( 1 - \frac{\lambda}{3} \right) \quad (21)$$

For small values of  $\lambda$ , a similar expression is obtained for copolymers with tanh gradients:

$$\mu_{\chi 0}(\text{tanh}) = \chi(1 - f)N_c \left( 1 - \frac{\lambda}{2} \right) \quad (22)$$

Equation 22 is valid for  $\lambda < 0.5$ . For larger values of  $\lambda$ ,  $\mu_{\chi 0}$  can be obtained by numerical integration. These values are shown as the symbols in Figure 2 for  $f = 0.5$ , where they are compared: eq 21 (solid line) and eq 22 (dashed line). The rounding of the tanh gradient profiles in comparison to the linear gradient profiles gives a larger value of  $\mu_{\chi 0}$  than a linear gradient for the same

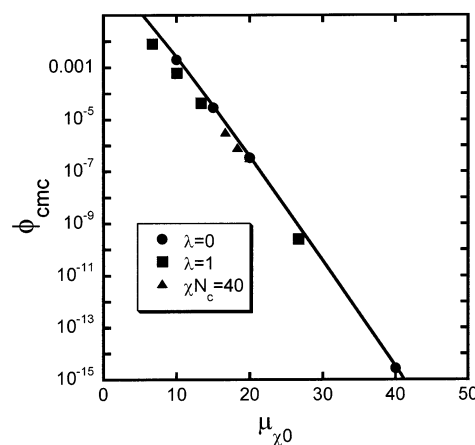


**Figure 3.** Critical micelle concentration for a series of copolymers with linear gradients, with  $f = 0.5$  and  $N_c/N_h = 1$ .

value of  $\lambda$ . In effect, the tanh gradient copolymers behave as linear gradient polymers with a slightly increased value of  $\lambda$ .

Equation 17 and eq 20 can be combined to give  $\phi_{\text{cmc}}$  as a function of  $\mu_{\chi 0}$ , which is a measure of the thermodynamic incompatibility between the gradient copolymer and the homopolymer matrix in which it resides. The result of this calculation for linear gradients with  $f = 0.5$  is shown as the solid line in Figure 3 and is in good agreement with the SCF results obtained by numerical solution of the equations in section 2. For these copolymers with linear gradients,  $\mu_{\chi 0}$  is given by  $(1 - f)\chi N_c(1 - \lambda/3)$  (eq 21). These calculations were carried out for standard diblock copolymers with  $\lambda = 0$  (circles), for fully tapered diblock copolymers with  $\lambda = 1$  (squares), and for a series of copolymers where  $(1 - f)\chi N_c$  is fixed at 20, but where  $\lambda$  varies between 0 and 1 (triangles). The analytic expressions represented by the solid line are exceptionally accurate for diblock copolymers with  $\lambda = 0$ , but overestimate the copolymer chemical potential by about  $1.6k_B T$  for the tapered, linear gradient copolymers with  $\lambda = 1$ . As a result, the values of  $\phi_{\text{cmc}}$  for  $\lambda = 1$  are about a factor of 5 less than the values predicted by the analytic treatment. As discussed in more detail below, this chemical potential reduction can be attributed to the fact that composition gradients in the block copolymer molecules result in broad, low energy interfaces between A and B components that make up the "core" and "corona" portions of a micelle.

The extremely low values of  $\phi_{\text{cmc}}$  obtained for moderate values of  $(1 - f)\chi N_c$  are responsible for the limited utility of block copolymers as interfacial modifiers in actual applications. Equilibration of an interface is generally mediated by the diffusion of free copolymer chains, which are present at a volume fraction equal to  $\phi_{\text{cmc}}$ . Situations where block copolymers have been used to modify interfacial properties have generally involved systems with  $(1 - f)\chi N_c < 10$ , so that the copolymer molecules are able to diffuse to the interface on experimentally reasonable time scales.<sup>2,3</sup> The exponential dependence on  $(1 - f)\chi N_c$  for the diffusion coefficient of block copolymer molecules in ordered morphologies is a related phenomenon.<sup>36-38</sup> The data in Figure 3 indicate that this same limitation exists for gradient copolymers as well, although slightly longer molecules can be used because of the increased solubility of gradient copolymers in the matrix phase, which appears in the present analysis through the introduction of a

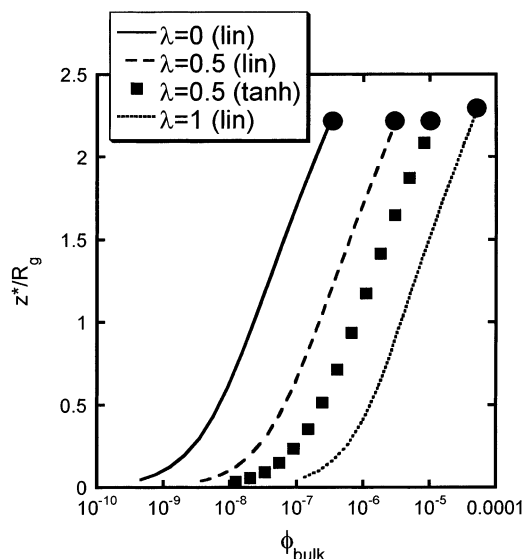


**Figure 4.** Series of adsorption isotherms for different values of  $\lambda$ , with  $N_c/N_h = 1$  and  $\chi N_c = 40$ .

factor of  $(1 - \lambda/3)$  in the expression for the copolymer chemical potential.

When appropriately normalized as described here, many of the interfacial properties of gradient copolymers are independent of the composition gradient described by  $\lambda$ . These properties include the segregation of copolymer molecules to the interface between A and B homopolymer phases. A useful measure of the number of block copolymer molecules in the interfacial layer is the integrated copolymer volume fraction,  $z^*$ , defined in the following way

$$z^* = \int_{-\infty}^{\infty} \{\phi_c(z) - \phi_{\text{bulk}}(z)\} dz \quad (23)$$

where  $\phi_{\text{bulk}}(z > 0)$  is the equilibrium volume fraction of copolymer in the B phase and  $\phi_{\text{bulk}}(z < 0)$  is the equilibrium volume fraction of copolymer in the A phase. For the symmetric copolymers studied in this paper, both of these bulk volume fractions are equal to one another.

Figure 4 is a comparison of adsorption isotherms for four symmetric copolymers ( $f = 0.5$ ), each with  $\chi N_c = 40$ . One of the copolymers is a traditional block copolymer ( $\lambda = 0$ ), one is a fully tapered linear gradient copolymer ( $\lambda = 1$ ), and the last two are linear and tanh gradient copolymers with  $\lambda = 0.5$ . The horizontal offset between the isotherms with  $\lambda = 1$  and  $\lambda = 0$  is consistent with the factor of  $(1 - \lambda/3)$  in the expression relating  $\phi_{\text{bulk}}$  to the copolymer chemical potential and with the fact that, for a given value of  $z^*$ , the copolymer chemical potential in the copolymer layer with  $\lambda = 1$  is about  $1.6k_B T$  less than for the copolymer with  $\lambda = 0$ . The linear gradient copolymer with  $\lambda = 0.5$  has intermediate properties, with a copolymer chemical potential that is about  $1.1k_B T$  less than that for the copolymer with  $\lambda = 0$ . Most of the difference between the adsorption isotherms for linear and tanh gradient copolymers with  $\lambda = 0.5$  can be attributed to the greater solubility of the tanh gradient copolymers in the homopolymer matrix, due to the lower value of  $\mu_{\gamma 0}$  (compare eqs 21 and 22). The chemical potentials for these two copolymers at a fixed value of  $z^*$  differ by only  $0.26k_B T$ , with the tanh gradient copolymer having the lower value. This result supports the general conclusion that the tanh gradient

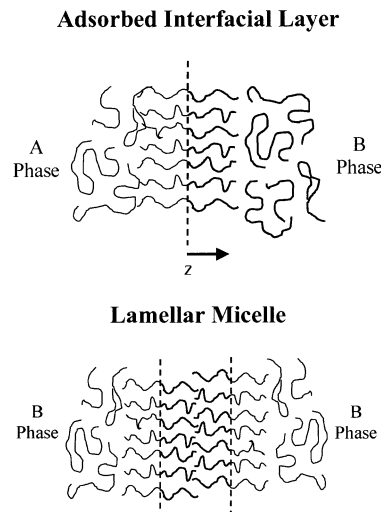


**Figure 5.** Schematic illustration of diblock copolymers at the interface between A and B homopolymers (top), and of a lamellar micelle in a matrix of B homopolymer (bottom). Dotted lines correspond to interfaces between A and B repeat units.

copolymers behave as linear gradient copolymers with a slightly larger value of  $\lambda$ . Subsequent discussion is therefore confined to the behavior of linear gradient copolymers, without a substantial loss of generality.

The end point of each isotherm corresponds to the case where the interfacial tension between the two phases has been reduced to 0. It is useful here to recall the Gibbs adsorption equation, which relates the equilibrium copolymer excess to the decrease in the interfacial free energy:

$$\gamma(\mu_c) = \gamma_0 - \frac{1}{N_c v_0} \int_{-\infty}^{\mu_c} z^*(\mu'_c) d\mu'_c \quad (24)$$

where  $\gamma_0$  is the interfacial free energy for the A/B interface in the absence of copolymer. For very high molecular weight homopolymers ( $\chi N_h \rightarrow \infty$ ),  $\gamma_0$  reaches an asymptotic limit given originally by Helfand and Tagami.<sup>39</sup> One is generally interested in smaller values of  $\chi N_h$ , however, where corrections to this asymptotic value become important.<sup>40</sup> The actual value of  $\gamma_0$  for the interface between monodisperse homopolymers of equal molecular weight can be calculated from the full self-consistent field theory<sup>26</sup> and is accurately described by the following analytic form suggested originally by Tang and Freed.<sup>41</sup>

$$\gamma_0 = \frac{ak_B T}{v_0} (\chi/6)^{1/2} \left\{ 1 - \frac{1.8}{\chi N_h} - \frac{0.4}{(\chi N_h)^2} \right\}^{3/2} \quad (25)$$

The similarity in shape of the adsorption isotherms plotted in Figure 4 shows that the interfacial behaviors of these two copolymers are very similar, and that the dependence of the interfacial activity of the copolymer molecules on  $\lambda$  is adequately described by any single point on the adsorption isotherm. A useful reference point is the end point of the isotherm at  $\phi_{\text{bulk}} = \phi_\gamma$ , where the interfacial free energy vanishes. Values of  $\phi_\gamma$  and  $\phi_{\text{cmc}}$  are closely related to one another, which becomes apparent when considering the similarities between the structure of an adsorbed copolymer layer and of a lamellar micelle. As illustrated in Figure 5, a lamellar micelle consists of two A/B interfaces that are placed

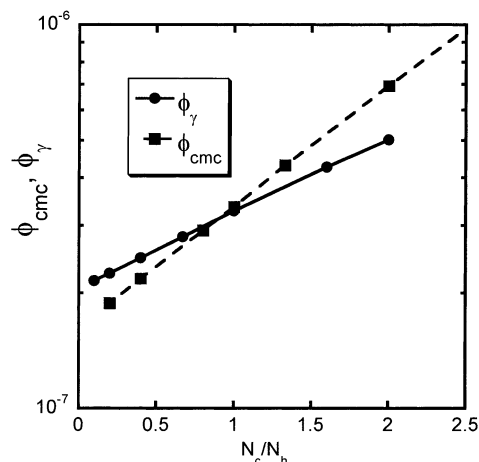


**Figure 6.** Critical volume fractions as a function of  $N_c/N_h$  for  $\lambda = 0$  and  $\chi N_c = 40$ . Linear gradients are assumed in all cases.

back to back. Micelles form when the free energy required to create these two interfaces vanishes, a condition that is very similar to the condition for which  $\gamma = 0$  for a single A/B interface. Within the approximations of the scaling treatment on which eq 17 is based,  $\phi_{cmc}$  and  $\phi_\gamma$  are identical to one another. More subtle effects associated with the entropy of the homopolymer molecules cause  $\phi_{cmc}$  and  $\phi_\gamma$  to differ from one another by a slight amount that depends on  $N_c/N_h$  and that can be calculated from the full SCF theory. The values of  $\phi_{cmc}$  and  $\phi_\gamma$  both increase as  $N_h$  is reduced, but  $\phi_\gamma$  increases faster than  $\phi_{cmc}$ . This effect is illustrated in Figure 6 for a symmetric diblock copolymer with  $\chi N_c = 40$  and  $\lambda = 0$ . For  $N_c/N_h < 0.9$ ,  $\phi_{cmc}$  is less than  $\phi_\gamma$ , so that copolymer micelles will form before the interfacial tension reaches 0. For high molecular weight homopolymers, individual micelles will condense to form an ordered microdomain morphology as opposed to a “microemulsion” phase consisting of A and B homopolymer phases that are stabilized with a layer of diblock copolymers.<sup>42</sup> This result can be understood in terms of attractive interactions between polymer “brushes”, so that multilayers such as those appearing in an ordered lamellar morphology or an isolated copolymer micelle are thermodynamically favored in comparison to isolated brushes. As described previously, these attractions emerge for values of  $N_c/N_h$  that are less than approximately 1.<sup>43,44</sup>

The similarity between  $\phi_{cmc}$  and  $\phi_\gamma$  is maintained for all values of  $\lambda$  between 0 and 1. This result is illustrated in Figure 7, where  $\phi_{cmc}$  and  $\phi_\gamma$  are plotted as a function of  $\lambda$  for linear gradient copolymers with  $f = 0.5$ ,  $N_c/N_h = 1$ , and  $\chi N_c = 40$ . The analytic prediction obtained from eqs 20 and 21, with  $\mu_{cmc} = 5.23 k_B T$  as obtained from eq 17, is represented by the dotted line in Figure 7. The increasing difference between this prediction and the more accurate values calculated from the SCF theory is due to the decrease in  $\mu_{cmc}$  as  $\lambda$  is increased from 0.

The differences between the structure of the adsorbed copolymer layer for  $\lambda = 0$  and  $\lambda = 1$  are illustrated in Figures 8 and 9. Figure 8 compares the volume fraction profiles for the A and B repeat units originating from the copolymer. Note that the distance scale is normalized by  $R_g$ , the radius of gyration of the copolymer, given by  $a(N_c/6)^{1/2}$ . For  $\lambda = 0$ , the A and B portions of the diblock copolymer form distinct brushes, with very little overlap between the volume fraction profiles originating from the A and B blocks.<sup>20</sup> The inherent composition

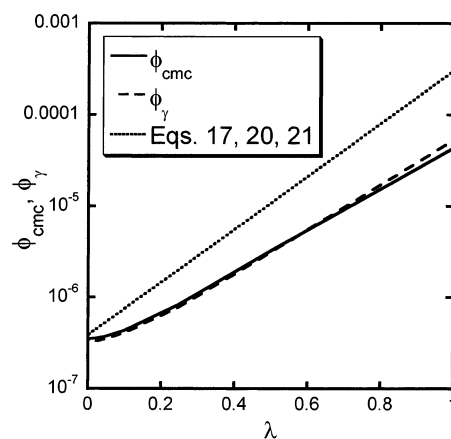


**Figure 7.** Critical volume fractions as a function of  $\lambda$  for linear gradient copolymers with  $f = 0.5$ ,  $N_c/N_h = 1$  and  $\chi N_c = 40$ .

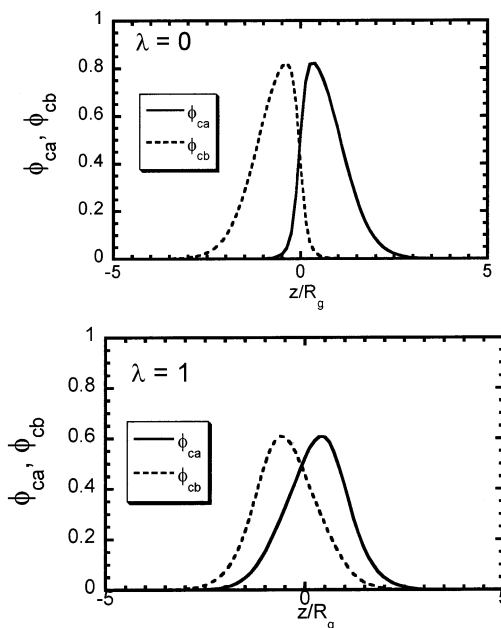


**Figure 8.** Concentration profiles corresponding to A and B repeat units originating from copolymer with linear gradients, localized at the interface between A and B homopolymers for  $f = 0.5$ ,  $N_c/N_h = 1$  and  $\chi N_c = 40$ .

variation within the gradient copolymers results in a much broader interface, with a wider overlap of the profiles corresponding to A and B repeat units. The breadth of this interface is more clearly demonstrated by plotting the overall distribution of A and B repeat units in the system. These distributions are illustrated in Figure 9 (symbols), along with the fits to the following hyperbolic tangent expression commonly used to describe interfacial widths in polymer systems (lines):

$$\phi_a(z) = 0.5 + 0.5 \tanh(2z/w), \quad \phi_b(z) = 1 - \phi_a(z) \quad (26)$$

For  $\lambda = 0$ , the interfacial width,  $w$ , is slightly larger than the asymptotic value obtained for the interface between polymers with very high molecular weight.<sup>45</sup> This limiting value of the interfacial width, referred to here as  $w_\infty$ , was obtained originally by Helfand and Tagami<sup>39</sup> and can be written in either of the following forms:

$$w_\infty = \frac{2a}{(6\chi)^{1/2}}, \quad \frac{w_\infty}{R_g} = \frac{2}{(\chi N_c)^{1/2}} \quad (27)$$

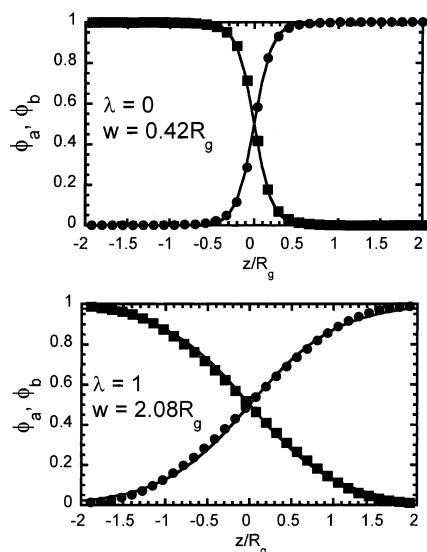


**Figure 9.** Overall volume fraction profiles of A and B repeat units for the same conditions used to generate the data in Figure 8.

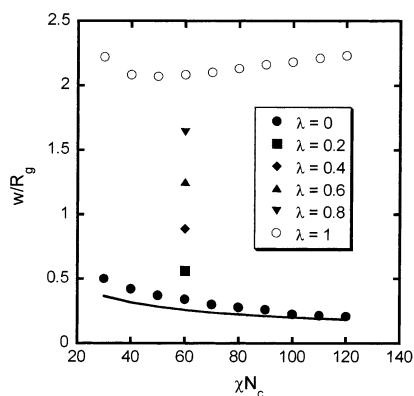


**Figure 10.** Interfacial width, normalized by the copolymer radius of gyration, as a function of  $\chi N_c$  for copolymers with linear gradients at the interface between immiscible homopolymers, for  $N_c/N_h = 1$  and  $\phi_{\text{bulk}} = \phi_g$ .

The key difference between the interfacial properties of traditional block copolymers and gradient copolymers is that the zone of mixing between A and B repeat units is controlled by the copolymer radius of gyration, and not by the thermodynamic incompatibility between the repeat units. This result is illustrated in Figure 10, where the normalized interfacial width is plotted as a function of  $\chi N_c$  for  $\lambda = 0$  and  $\lambda = 1$ . The asymptotic form for highly immiscible homopolymers (eq 27) is included for comparison (solid line). As with the profiles shown in Figures 8 and 9, the data in this figure correspond to an adsorbed copolymer under conditions where  $\gamma = 0$  ( $\phi_{\text{bulk}} = \phi_g \approx \phi_{\text{cmc}}$ ), and are representative of the interfacial widths that exist within lamellar micelles, and within a periodic phase that can be viewed as a system of condensed lamellar micelles. For  $\lambda = 1$ , the interfacial width is about twice the copolymer radius of gyration, with very little dependence on  $\chi N_c$ . The interfacial widths for  $\lambda = 0$  are larger than the predictions of eq 27, a result that can be attributed to the entropic penalty associated with the confinement of the joint between copolymer blocks to the interfacial region.<sup>45</sup> Values of  $w$  for  $\lambda = 0$  can be expressed in terms of  $w_\infty$  by introducing a correction factor,  $A_w$ , which decreases from 1.4 for  $\chi N_c = 30$  to about 1.1 at  $\chi N_c = 120$ , and which continues to decrease asymptotically

toward 1.0 as  $\chi N_c$  increases further:

$$w(\lambda = 0) = A_w(\chi N_c) w_\infty \quad (28)$$

As  $\lambda$  increases from 0 to 1,  $w$  increases from  $A_w w_\infty$  to a value that is close to twice the copolymer radius of gyration. As illustrated by the data included in Figure 10 for  $\chi N_c = 60$ , this increase in width is roughly linear in  $\lambda$ , so the following approximate expression for the interfacial width describes the distribution of A and B segments across the interface.

$$w \approx A_w(\chi N_c) w_\infty + 2\lambda R_g \quad (29)$$

The increased value of the A/B interfacial width, and the coupling of this width with the radius of gyration of the copolymer molecule, is the distinctive feature of the interfacial behavior of gradient copolymers. A variety of interesting implications arise from this enhanced ability to control the composition modulation. If the A and B components have very different glass transition temperatures, for example, a material with an exceptionally broad glass transition can be obtained. This property could be very useful in the design of materials for vibration damping. An increased interfacial width also has mechanical implications for the strength of the interface between glassy polymers, since a single molecule is expected to be able to make multiple entanglements with both phases. The situation is similar to the ability of random copolymers to strengthen the interface between glassy polymers.<sup>46,47</sup> Statistical copolymers typically form wetting layers at the interface between the corresponding homopolymers, however, and the thickness of these wetting layers is not limited to a single monolayer.<sup>48</sup> Gradient copolymers provide a mechanism for tailoring the interfacial width between A and B segments from a single copolymer monolayer that is localized at the interface.

#### 4. Conclusions

The interfacial behavior of gradient copolymers is qualitatively similar to the behavior that has been observed for traditional block copolymers, in that A/B gradient copolymers segregate preferentially to the interface between A and B homopolymers. Above a critical concentration of free copolymer chains corresponding to the formation of micellar aggregates, the copolymer chemical potential remains fixed. The addition of more copolymer to the system produces additional micelles without affecting the interfacial structure. A detailed study of the interfacial structure has been carried out utilizing numerical self-consistent field theory, modified from previous versions to take into account a smoothly varying composition gradient along the copolymer chain. These equations have been solved for a symmetric copolymer containing equal amounts of A and B repeat units characterized by different values of the gradient parameter  $\lambda$  that varied from 0 (for a traditional diblock copolymer) to 1 (for a fully tapered gradient copolymer). The following conclusions have been obtained:

- (1) The copolymer chemical potential at the micelle transition decreases as  $\lambda$  increases. For symmetric copolymers with  $\chi N_c = 40$ , this chemical potential is about  $1.6 k_B T$  lower for  $\lambda = 1$  than it is for  $\lambda = 0$ .
- (2) Emulsified phases, corresponding to a vanishing interfacial free energy between the homopolymer phases,



can be obtained for all values of  $\lambda$  between 0 and 1, provided that the homopolymer molecular weight is sufficiently low. Ordered domain morphologies, corresponding to the condensation of micelles, are preferred for homopolymer molecular weights that exceed the copolymer molecular weight. The attractive interactions between micelles that are responsible for this condensation depend weakly on the value of  $\lambda$ . As  $\lambda$  is increased, the attractive interactions between micelles appear at slightly lower values of the homopolymer molecular weight.

(3) For a fully tapered gradient copolymer ( $\lambda = 1$ ), the composition profile corresponding to A or B repeat units within a copolymer micelle, within a periodic lamellar phase, or across an emulsified interface between immiscible polymers is controlled by the copolymer radius of gyration, with very little dependence on the thermodynamic incompatibility between A and B repeat units. For a fixed value of  $N_c$ , this interfacial width increases linearly with  $\lambda$ , and is equal to about twice the copolymer radius of gyration for  $\lambda = 1$ .

**Acknowledgment.** This work was supported by the MRSEC program of the National Science Foundation (DMR-0076097) at the Materials Research Center of Northwestern University.

## Appendix

The quadratic form for the fields given in eq 14 differs from the linear form that is often used. Nevertheless this formalism is entirely consistent with the work of Helfand,<sup>21,39,49,50</sup> Scheutjens, Fleer et al.,<sup>51,52</sup> Hong and Noolandi,<sup>53–56</sup> and others, where the linear form has been employed. This equivalence can be demonstrated by writing the fields for a binary system of incompressible A and B homopolymers in the following generalized form, where planar symmetry has been assumed:

$$\omega_a(z) = \chi\phi_b(z) - \Delta\omega(z) + K(z), \quad \omega_b(z) = \chi\phi_a(z) - \Delta\omega(z) + K(z) \quad (30)$$

The corresponding generalized expression for the interfacial free energy is as follows:

$$\gamma = \frac{k_B T a}{v_0} \int \left\{ \Delta\omega(z) - \chi\phi_a(z)\phi_b(z) + \frac{\phi_a(z)}{N_a} + \frac{\phi_b(z)}{N_b} - K(z) \right\} dz \quad (31)$$

The linear and quadratic forms for the fields arise from different choices that are made in the specification of  $K(z)$ . Note that the difference between the mean fields for A and B repeat units is the same for all possible values of  $K(z)$ , and is linear in the composition variation:

$$\omega_a(z) - \omega_b(z) = \chi(\phi_b(z) - \phi_a(z)) \quad (32)$$

The equations used here correspond to the following choice for  $K(z)$ , chosen so that the fields have forms that are similar to the Flory–Huggins expressions for the chemical potentials:

$$K(z) = -\chi\phi_a(z)\phi_b(z) + \frac{\phi_a(z)}{N_a} + \frac{\phi_b(z)}{N_b} \quad (33)$$

With this choice for  $K(z)$ , and with  $\phi_a + \phi_b = 1$ , one

obtains the following expressions for the fields:

$$\begin{aligned} \omega_a(z) &= \chi\phi_b^2(z) - \Delta\omega(z) + \frac{\phi_a(z)}{N_a} + \frac{\phi_b(z)}{N_b} \\ \omega_b(z) &= \chi\phi_a^2(z) - \Delta\omega(z) + \frac{\phi_a(z)}{N_a} + \frac{\phi_b(z)}{N_b} \end{aligned} \quad (34)$$

These equations are specific forms of eq 14. Expressing the fields in terms of the chemical potential expressions simplifies the extension to systems with additional components, as has been described previously.<sup>20,26</sup>

## References and Notes

- (1) Fayt, R.; Jérôme, R.; Teyssie, P. *Polym. Eng. Sci.* **1987**, *27*, 328.
- (2) Anastasiadis, S. H.; Gancarz, I.; Koberstein, J. T. *Macromolecules* **1989**, *22*, 1449.
- (3) Shull, K. R.; Kramer, E. J.; Hadzioannou, G.; Tang, W. *Macromolecules* **1990**, *23*, 4780.
- (4) Leibler, L. *Makromol. Chem., Macromol. Symp.* **1988**, *16*, 1.
- (5) Bates, F. S.; Fredrickson, G. H. *Annu. Rev. Physiol. Chem.* **1990**, *41*, 525.
- (6) Kinning, D. J.; Winey, K. I.; Thomas, E. L. *Macromol.* **1988**, *21*, 3502.
- (7) Winey, K. I.; M. I. T., 1991.
- (8) Winey, K. I.; Thomas, E. L.; Fetters, L. J. *J. Chem. Phys.* **1991**, *95*, 9367.
- (9) Winey, K. I.; Thomas, E. L.; Fetters, L. J. *Macromolecules* **1992**, *25*, 2645.
- (10) Wang, J. S.; Matyjaszewski, K. *Macromolecules* **1995**, *28*, 7901.
- (11) Patten, T. E.; Matyjaszewski, K. *Adv. Mater.* **1998**, *10*, 901.
- (12) Matyjaszewski, K.; Xia, J. *Chem. Rev.* **2001**, *101*, 2921.
- (13) Malmstrom, E. E.; Hawker, C. J. *Macromol. Chem. Phys.* **1998**, *199*, 923.
- (14) Hawker, C. J.; Barclay, G. G.; Orellana, A.; Dao, J.; Devonport, W. *Macromolecules* **1996**, *29*, 5245.
- (15) Gray, M.; Nguyen, S.; Zhou, H.; Torkelson, J. M. *Polym. Prepr.* **2002**.
- (16) Evers, O. A.; Scheutjens, J. M. H. M.; Fleer, G. J. *Macromolecules* **1990**, *23*, 5221.
- (17) ten Brinke, G.; Karasz, F. E.; MacKnight, W. J. *Macromolecules* **1983**, *16*, 1827.
- (18) *Polymer Phase Separation*; Sanchez, I. C.; Ed.; Academic Press: Orlando, FL, 1987; Vol. 11.
- (19) Matsen, M. W. *J. Phys.: Condens. Matter* **2002**, *14*, R21.
- (20) Shull, K. R.; Kramer, E. J. *Macromolecules* **1990**, *23*, 4769.
- (21) Helfand, E. *J. Chem. Phys.* **1975**, *62*, 999.
- (22) Donley, J. P.; Wu, D. T.; Fredrickson, G. H. *Macromolecules* **1997**, *30*, 2167.
- (23) Wu, D. T.; Fredrickson, G. H.; Carton, J.-P.; Ajdari, A.; Leibler, L. *J. Polym. Sci., Part B: Polym. Phys.* **1995**, *33*, 2373.
- (24) Donley, J. P.; Rajasekaran, J. J.; McCoy, J. D.; Curro, J. G. *J. Chem. Phys.* **1995**, *103*, 5061.
- (25) Bruder, F.; Brenn, R. *Macromolecules* **1991**, *24*, 5552.
- (26) Shull, K. R. *Macromolecules* **1993**, *26*, 2346.
- (27) Leibler, L. *Macromolecules* **1980**, *13*, 1602.
- (28) Aksimentiev, A.; Holyst, R. *J. Chem. Phys.* **1999**, *111*, 2329.
- (29) Fredrickson, G. H.; Helfand, E. *J. Chem. Phys.* **1987**, *87*, 697.
- (30) Bates, F. S.; Rosedale, J. H.; Fredrickson, G. H.; Glinka, C. J. *Phys. Rev. Lett.* **1988**, *61*, 2229.
- (31) Fredrickson, G. H.; Milner, S. T. *Phys. Rev. Lett.* **1991**, *67*, 835.
- (32) Fredrickson, G. H.; Milner, S. T.; Leibler, L. *Macromolecules* **1992**, *25*, 6341.
- (33) Matyjaszewski, K. *J. Macromol. Sci.—Pure Appl. Chem.* **1997**, *10*, 1785.
- (34) Pakula, T. *Macromol. Theory Simul.* **1996**, *5*, 987.
- (35) Dai, K. H.; Kramer, E. J.; Shull, K. R. *Macromolecules* **1992**, *25*, 220.
- (36) Yokoyama, H.; Kramer, E. J. *Macromolecules* **1998**, *31*, 7871.
- (37) Yokoyama, H.; Kramer, E. J. *Macromolecules* **2000**, *33*, 954.
- (38) Yokoyama, H.; Kramer, E. J.; Fredrickson, G. H. *Macromolecules* **2000**, *33*, 2249.
- (39) Helfand, E.; Tagami, Y. *J. Chem. Phys.* **1972**, *56*, 3592.
- (40) Broseta, D.; Fredrickson, G. H.; Helfand, E.; Leibler, L. *Macromolecules* **1990**, *23*, 132.



- (41) Tang, H.; Freed, K. F. *J. Chem. Phys.* **1991**, *94*, 6307.
- (42) Matsen, M. W. *J. Chem. Phys.* **1999**, *110*, 4658.
- (43) Shull, K. R. *J. Chem. Phys.* **1991**, *94*, 5723.
- (44) Ferreira, P. G.; Ajdari, A.; Leibler, L. *Macromolecules* **1998**, *31*, 3994.
- (45) Shull, K. R. *Macromolecules* **1992**, *25*, 2122.
- (46) Dai, C. A.; Dair, B. J.; Dai, K. H.; Ober, C. K.; Kramer, E. J.; Hui, C. Y.; Jelinski, L. W. *Phys. Rev. Lett.* **1994**, *73*, 2472.
- (47) Creton, C.; Kramer, E. J.; Brown, H. R.; Hui, C.-Y. *Adv. Polym. Sci.* **2002**, *53*.
- (48) Lee, M. S.; Lodge, T. P.; Macosko, C. W. *J. Polym. Sci., Part B: Polym. Phys.* **1997**, *35*, 2835.
- (49) Helfand, E.; Tagami, Y. *J. Chem. Phys.* **1972**, *57*, 1812.
- (50) Helfand, E. *Macromolecules* **1975**, *8*, 552.
- (51) Evers, O. A.; Scheutjens, J. M. H. M.; Fleer, G. J. *J. Chem. Soc., Faraday Trans.* **1990**, *86*, 1333.
- (52) Fleer, G. J.; Stuart, M. A. C.; Scheutjens, J. M. H. M.; Cosgrove, T.; Vincent, B. *Polymers at Interfaces*; Chapman and Hall: London, 1993.
- (53) Hong, K. M.; Noolandi, J. *Macromolecules* **1981**, *14*, 736.
- (54) Hong, K. M.; Noolandi, J. *Macromolecules* **1981**, *14*, 727.
- (55) Noolandi, J.; Hong, K. M. *Macromolecules* **1982**, *15*, 482.
- (56) Noolandi, J.; Hong, K. M. *Macromolecules* **1984**, *17*, 1531.

MA020698W